TECHNICAL PAPER

JOURNAL OF THE SOUTH AFRICAN INSTITUTION OF CIVIL ENGINEERING
ISSN 1021-2019 (print) | ISSN 2309-8775 (online)
Vol 65 No 2, June 2023, Pages 28–38, Paper 1492

Advanced numerical modelling of the nonlinear mechanical behaviour of a laterally loaded pile embedded in stiff unsaturated clay

K T Braun, N Bakas, G Markou, S W Jacobsz

Capturing and understanding the ultimate limit state behaviour of reinforced concrete piles embedded in soil requires the use of advanced tools or the performance of expensive tests. An experiment was performed where reinforced concrete piles embedded in a stiff unsaturated clay profile were load-tested on-site. However, even though in-situ experiments can provide engineers with valuable insight, their cost and time limitations come with restrictions, especially when dealing with a parametric investigation on the soil's material properties, the size of the piles, or the piles' material properties. The objective of this research work was to numerically model the nonlinear mechanical behaviour of laterally loaded full-scale piles through detailed 3D modelling, and perform an in-depth parametric investigation to provide answers to unknown factors that the actual physical experiment could not answer. Furthermore, this work serves as a pilot project that will be used to pave the way in developing multiple soil-structure interaction models that will be used to generate a dataset that helps the creation of predictive models through machine learning algorithms. For the needs of this research work, the reinforced concrete piles were discretised with 8-noded isoparametric hexahedral elements that accounted for cracking through the smeared crack approach. Steel reinforcement bars and stirrups were simulated as embedded rebar elements, while the soil domain was also discretised through 8-noded hexahedral elements. Most of the required material properties assumed during the nonlinear analyses were defined according to relevant laboratory experiments. According to the numerical investigation, it was found that the proposed numerical model has the ability to reproduce the experimental results with high accuracy, while providing in-depth insight on the failure mechanisms for both the soil and reinforced concrete domains.

INTRODUCTION

Piled foundations are commonly used to support structures in loose or soft soils, as shallow foundations are known for their inability to avoid extreme settlements and shear failure when used in such soil domains. Piles can either be subjected to vertical loads, lateral loads, or a combination of vertical and lateral loads. Karthigeyan *et al* (2006) mentioned that it is complex to analyse piles under combined loading, and therefore the load cases should be modelled independently. A vertical load analysis is used to determine the bearing capacity and settlement, while a lateral load analysis is used to determine the flexural behaviour. According to Červenka and Papanikolaou (2008) the methods to study the behaviour of piles subjected to lateral loading can be categorised into:

1. limit state methods
2. subgrade reaction methods
3. elastic continuum approaches
4. p-y methods
5. finite element methods.

In soil modelling, the combination of elasticity, plasticity and friction are options when modelling soil behaviour. Atkinson (2017) states that these combinations can

KEVIN BRAUN received his BEng and BEngHons at the University of Pretoria and is currently completing his MEng in Civil Engineering (Structures). His research work consists of modelling multiple soil-structure interaction models of a singular pile embedded in soil, where formulas using AI (artificial intelligence) and machine learning algorithms will be able to predict the failure force and horizontal displacement of a laterally loaded pile.

Contact details:
Department of Civil Engineering, University of Pretoria
Private Bag X20, Hatfield, Pretoria 0028, South Africa
E: u17031215@tuks.co.za

DR NIKOLAOS BAKAS is a Senior Data Scientist at the National Infrastructures for Research and Technology, GRNET. He has been a lecturer at Neapolis University Pafos, and an Associate Research Scientist at the Computation-based Science and Technology Research Center, at The Cyprus Institute. His research interests comprise the fundamental mathematical modelling of machine learning algorithms, as well as applications in a variety of thematic areas. Apart from research, he has been a PI for multiple industrial applications of AI (artificial intelligence).

Contact details:
National Infrastructures for Research and Technology – GRNET
7 Kifisias Avenue, Athens 11523, Greece
E: nibas@grnet.gr

PROF GEORGE MARKOU received his PhD degree at the National Technical University of Athens, Greece. His speciality involves numerous scientific fields related to the modelling of structures through the use of the finite element method. His recent research work addresses the modelling of composite structures under seismic loading conditions, soil-structure interaction problems, assessment of retrofitted structures, smart monitoring of structures, and the use of machine learning algorithms for solving engineering problems. Prof Markou is also using high-performance computing in the development of predictive models through machine learning algorithms. He is currently an Associate Professor at the University of Pretoria in the Department of Civil Engineering.

Contact details:
Department of Civil Engineering, University of Pretoria
Private Bag X20, Hatfield, Pretoria 0028, South Africa
E: george.markou@up.ac.za

PROF SW JACOBSZ completed BEng and MEng degrees at the University of Pretoria, and a PhD at the University of Cambridge. He was employed by Jones & Wagener Consulting Engineers as geotechnical engineer for ten years, and was then appointed as Associate Professor in the Department of Civil Engineering at the University of Pretoria in 2010. His research interests include physical modelling of geotechnical and soil-structure interaction problems and aspects related to unsaturated soil mechanics. He has been involved in several large-scale field trials, including large surcharge trials on residual dolomite, large-scale testing of piles in expansive clays and monitoring the in-situ state on a range of tailings dams

Contact details:
Department of Civil Engineering, University of Pretoria
Private Bag X20, Hatfield, Pretoria 0028, South Africa
E: sw.jacobsz@up.ac.za

Keywords: soil-structure interaction, reinforced concrete pile, soil domain, mechanical behaviour, finite element method

Braun KT, Bakas N, Markou G, Jacobsz SW. Advanced numerical modelling of the nonlinear mechanical behaviour of a laterally loaded pile embedded in stiff unsaturated clay. J. S. Afr. Inst. Civ. Eng. 2023:65(2), Art. #1492, 11 pages. http://dx.doi.org/10.17159/2309-8775/2023/v65n2a4

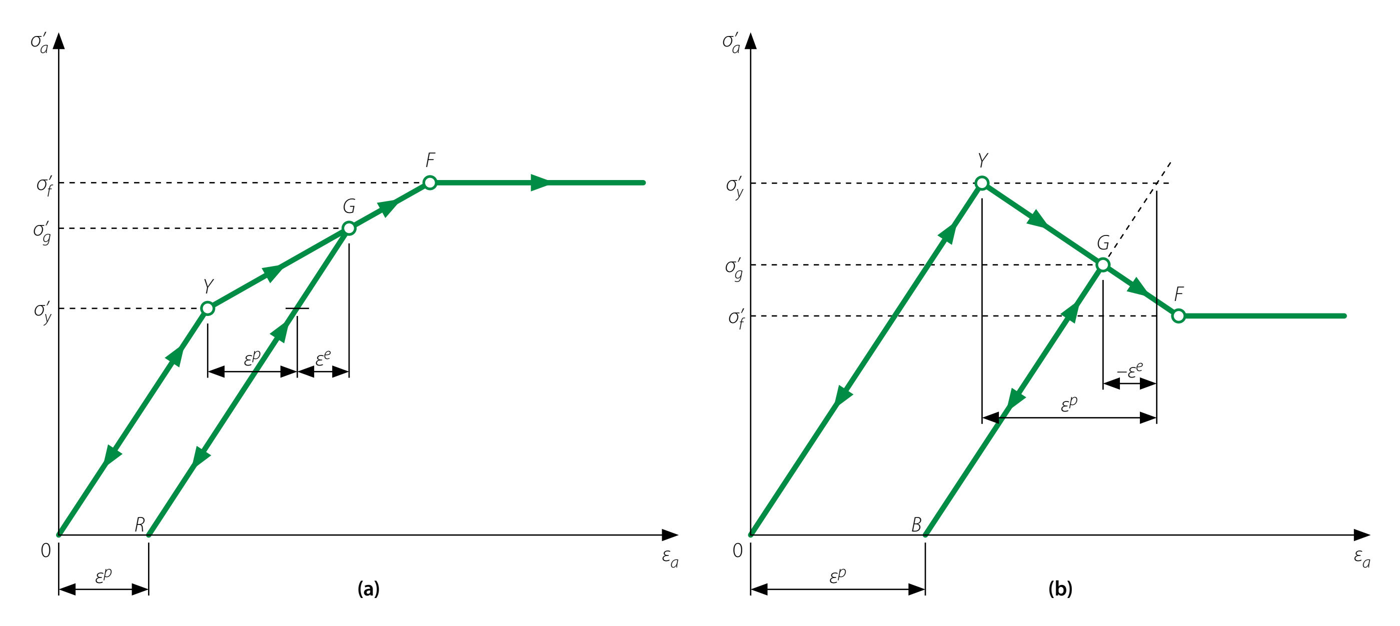

Figure 1 **Strain hardening (a) and strain softening (b) (adapted from Atkinson 2017)**

be combined into a single model known as the critical state model. Atkinson (2017) proves that by considering the stress-strain relationship of soils, they can typically behave in three different ways, namely: elastic-perfectly plastic, elastic-plastic hardening, and elastic-plastic softening. A perfectly plastic material continues to strain with constant stress, and therefore plastic deformation occurs during plastic deformation only. Hence, it does not experience elastic deformation under plastic strain. An elastic-plastic material that strain hardens experiences elastic strain during plastic deformation, while an elastic-plastic material that strain softens releases elastic strain during plastic deformation (Atkinson 2017). Figure 1 represents the stress-strain curves for an elastic-plastic strain hardening and softening material, respectively.

Jardine *et al* (1986) studied the influence of non-linear stress-strain experienced within soil-structure interaction (SSI) problems. It was stated that from field and laboratory studies, at very small strains, most soils experience a non-linear stress-strain behaviour. It was therefore concluded that, despite the treatment of soil as a linear elastic material in SSI problems, which represents an effective tool for expressing soil stiffness if non-linearities are not considered, the results can be misleading. Breysse *et al* (2005) investigated the effect of soil heterogeneity within SSI problems. Breysse *et al* (2005) showed that soil heterogeneity induces changes in the differential settlement, bending moments, stresses, and possibly cracking within the SSI problem which cannot be predicted if homogeneous conditions are assumed. Soil heterogeneity also induces stresses which are dependent on the soil variability, the soil-structure stiffness ratio, and the soil-structure length ratio (soil fluctuation scale and structural dimensions).

According to Kausel (2010), research work considering the early history of SSI describes the SSI phenomenon as somewhat difficult to define. This was because of the complex dynamic interactions due to the amplification of seismic waves present within the soil layers. Another research work analysed the non-linear behaviour of laterally loaded piles (Kavitha *et al* 2016), where they investigated the soil-pile interaction effect when loaded laterally. It was reported that the soil-pile interaction effect depended on the soil properties, loading type, ground slope, as well as the pile material and diameter (Kavitha *et al* 2016).

A study by Gravett and Markou (2021) performed a state-of-the-art investigation on wind turbine structures founded on soft clay, where SSI was also considered. This work investigated the interaction of soil and structural mechanics, and foresaw the derivation of an optimum pile foundation geometry based on modal and ultimate limit nonlinear pushover analyses. Gravett and Markou (2021) used ReconanFEA (2020) to perform the analyses in a detailed 3D approach to discretise, model and analyse numerous finite element (FE) models. They reported that the use of hexahedral finite elements was ideal for this type of SSI problem. It is noteworthy to refer to the recent research work by Gravett *et al* (2021), where the fundamental period of reinforced concrete (RC) buildings was investigated, which included SSI effects. In their research work, a digitally generated dataset was used to derive a closed-form formula that was able to accurately predict the fundamental period of RC buildings with and without accounting for the SSI effect. A similar approach that will foresee the use of artificial intelligence (AI) and machine learning algorithms will be used by the authors after the successful delivery of the research work discussed herein.

The finite element method (FEM) is one of the most commonly used numerical approaches in industry, as well as for research purposes. This method aims to predict the mechanical behaviour of structures, allowing and assisting engineers to numerically investigate structures. For this reason, the FEM-based software (ReconanFEA 2020) is used for the needs of this research work. Furthermore, by analysing numerical models under different loading conditions and using a variety of meshes, it can be determined if the structural design is safe or not (Markou & Roeloffze 2021). Modelling of piles embedded in soil was performed by Gravett and Markou (2021), where experimental and numerical results showed that ReconanFEA (2020) has the ability to objectively capture the mechanical response of this complex problem. Therefore, the modelling that was conducted herein to investigate the behaviour of piles subjected to different loading conditions follows a similar approach, adopting detailed 3D modelling of solid elements to discretise both the concrete and soil domains.

A research project which aimed to investigate the behaviour of piled foundations, particularly for wind turbines in partially saturated clay soils, was recently undertaken in South Africa. Expansive soils are located in many sub-arid and sub-humid parts across the African continent, and therefore the design of superstructures within or on expansive soils is critical for the future of the socio-economy of Africa. Field tests were carried out on a site near Vredefort in South Africa. This site was underlain by expansive clay which extends to depths in excess of 7 m, with bedrock occurring at about 15 m. Two sets of lateral pile load tests were conducted with the soil in a dry (in-situ) state, as well as after saturating the soil.

The objective of this study was to use advanced numerical models to analyse the nonlinear mechanical behaviour of RC piles embedded in clay by replicating in-situ lateral load tests. Concrete, steel and soil properties were modelled in the numerical analysis performed herein according to the material tests performed for the purposes of the physical experiment. However, for unknown properties, specific engineering judgement had to be used to obtain representative values, especially in the case of the soil. Thereafter, a sensitivity analysis was conducted on these material properties to determine how sensitive the assumptions of property values were in terms of the analysis. For this purpose, numerical software packages such as FEMAP (Ouanta *et al* 2016) were used. By developing models through FEMAP and analysing them through the use of the ReconanFEA software package, while considering the input parameters measured from the full-scale RC pile load research project in Vredefort, South Africa, correlations between the models and real-life experiments were performed. Additionally, even though the physical experiment did not proceed to ultimate failure, it is shown herein that the numerical simulations provided much missing information, complementing the physical experiment by answering questions such as revealing the failure mechanism, as well as the ultimate lateral load at which the RC pile failed.

MODELLING OF CONCRETE AND SOIL MATERIAL

Modelling in 3D considers the effect of out-of-plane stresses, where the stress-strain relationship for each stress-state is expressed by the hydrostatic (σ_0) and deviatoric components (τ_0) (Markou & Roeloffze 2021). The recent research work presented by Gravett and Markou (2021) describes how the corresponding hydrostatic and deviatoric strains (ε_0, γ_0) are used to produce the hydrostatic and deviatoric stresses, by using a material model proposed by Kotsovos and Pavlovic (1995) and extended by Markou and Papadrakakis (2013).

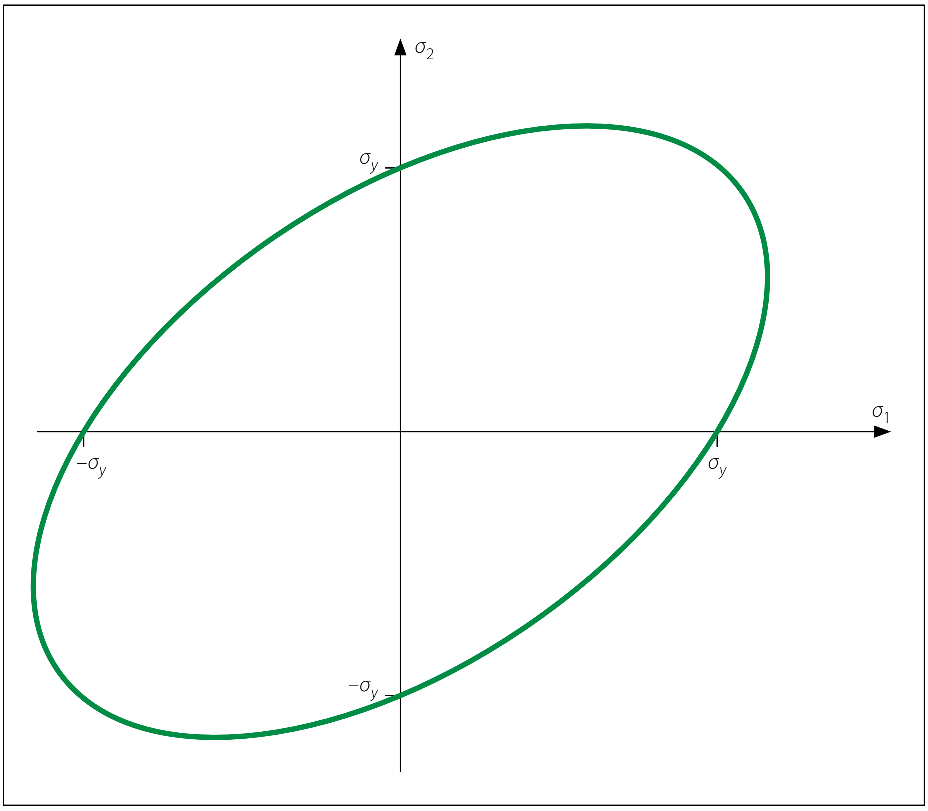

Figure 2 Von Mises 2D yielding criterion curve (adapted from Gravett & Markou 2021)

$$\varepsilon_0 = \varepsilon_{0h} + \varepsilon_{0d} = \frac{\sigma_0 + \sigma_{id}}{3K_S}, \ \gamma_0 = \frac{\tau_0}{2G_S} \tag{1}$$

In Equation 1, σ_{id} expressed as a function of (σ_0, τ_0, f_c) is an equivalent external stress, which accounts for the coupling effect between τ_0 and ε_{0d} (Gravett & Markou 2021). In addition, the bulk modulus K_S (σ_0, τ_0) and the shear modulus G_S (σ_0, τ_0) are obtained by ignoring σ_{id}. By considering the relationship in Equation 1, the strains in global coordinates are expressed as follows:

$$\varepsilon_{ij} = \frac{\sigma_{ij} + \sigma_{id}\delta_{ij}}{2G_S} - \frac{3v_S}{E_S}(\sigma_0 + \sigma_{id})\delta_{ij} \tag{2}$$

Where: δ_{ij} is the Kronecker delta, σ_{ij} and ε_{ij} are the total stresses and strains, respectively. E_S (σ_0, τ_0, f_c) and v_S (σ_0, τ_0, f_c) are the secant Young modulus and Poisson's ratio, respectively, which are derived from K_S and G_S (Markou & Roeloffze 2021). E_S and v_S are expressed as:

$$E_S = \frac{9K_SG_S}{3K_S + G_S}, \ v_S = \frac{3K_S - 2G_S}{6K_S + 2G_S} \tag{3}$$

The formulation that describes the strength envelope of concrete (Markou *et al* 2018) is expressed as:

$$\tau_{0u} = \frac{2\tau_{0c}(\tau_{0c}^2 - \tau_{0e}^2)\cos\theta + \tau_{0c}(2\tau_{0e} - \tau_{0c})\sqrt{4(\tau_{0c}^2 - \tau_{0e}^2)\cos^2\theta + 5\tau_{0e}^2 - 4\tau_{0c}^2\tau_{0e}^2}}{4(\tau_{0c}^2 - \tau_{0e}^2)\cos^2\theta + (2\tau_{0e} - \tau_{0c})^2} \tag{4}$$

This expression represents a smooth convex curve, where θ is the rotational angle between the deviatoric stress vector and one of the projected stress principal axis located on the deviatoric plane. In addition, once the failure criteria is satisfied, the smeared crack approach is imitated where macro-cracking occurs (Gravett & Markou 2021).

In terms of reinforcement modelling, the Menegotto-Pinto method, which also considers the Bauschinger effect, is integrated within the ReconanFEA software (Menegotto 1973). The stress-strain relationship for the steel material is presented as:

$$\sigma^* = b\varepsilon^* + \frac{(1 - b)\varepsilon^*}{(1 + \varepsilon^{*R})^{1/R}} \tag{5}$$

Where:

$$\varepsilon^* = \frac{\varepsilon - \varepsilon_r}{\varepsilon_0 - \varepsilon_r}, \tag{6}$$

$$\sigma^* = \frac{\sigma - \sigma_r}{\sigma_0 - \sigma_r}, \tag{7}$$

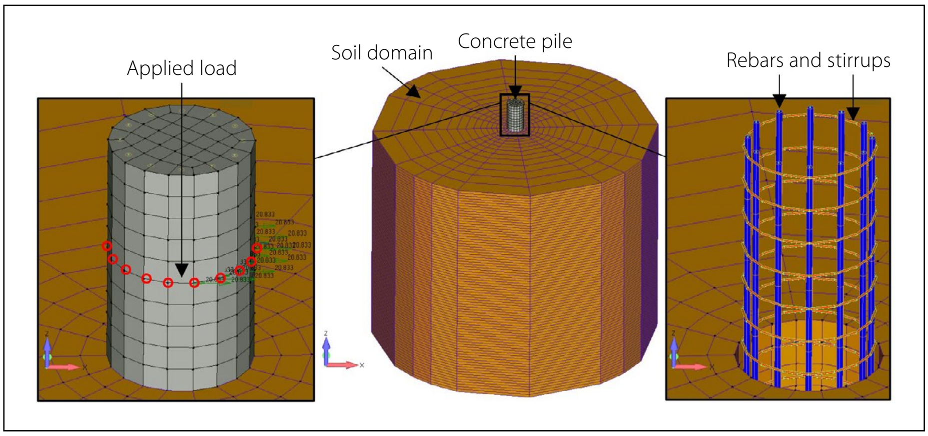

Figure 3 Finite element mesh of model 1 (left), load application (middle) and reinforcement details (right)

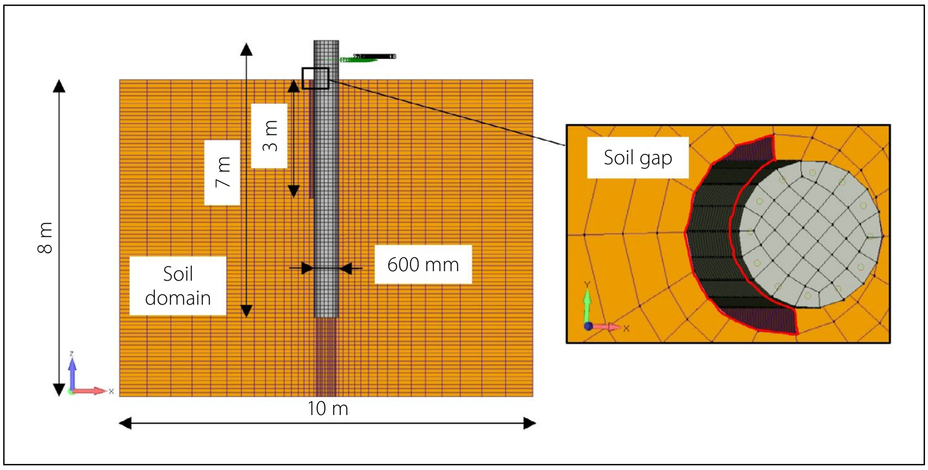

Figure 4 Finite element mesh of model 2; the interface of the pile and soil is detached

$$R = \frac{R_0 - a_1\xi}{\alpha_2 + \xi}, \tag{8}$$

Where: b is the strain hardening ratio, and ξ is the normalised plastic strain parameter. Furthermore, the parameters R_0, a_1 and a_2 are assumed parameters depending on the investigation of the problem at hand (Gravett & Markou 2021).

For the case of the soil domain that was discretised through the use of hexahedral elements, the adoption of a nonlinear elastoplastic 3D material model was performed that used a Von Mises yielding criterion described in Equation 9. The numerical investigation performed and presented in this research work foresaw that the RC pile is founded on unsaturated clay soil. It is also important to note here that the soil material model requires the definition of only three material properties – the E-value, Poisson's ratio, and the uniaxial ultimate strength. Figure 2 shows a typical Von Mises yielding criterion curve.

$$(\sigma_1 - \sigma_3)^2 - (\sigma_1 - \sigma_3)(\sigma_2 - \sigma_3) + (\sigma_2 - \sigma_3)^2 = \sigma_y^2 \tag{9}$$

SOIL STRUCTURE INTERACTION MODEL

The RC pile geometry used in the numerical analysis was developed based on the design of the field piles, where piles of 600 mm in diameter with lengths of 7 m were constructed. The pile was auto-discretised using hexahedral elements with an element size of 0.1 m. The soil surrounding the pile was modelled to a radius of 5 m and a depth of 8 m, while also being discretised with 8-noded isoparametric hexahedral elements. This first model (see Figure 3) assumed a full bond between the concrete-soil interface. The reinforcement of the pile (12Ø25 longitudinal and Ø10@150 stirrups) was also discretised and analysed in this study through the use of embedded rod elements that can be seen in Figure 3.

Given that the experiment foresaw the application of static loads, the soil domain was fixed at the bottom, and the nodes along the perimeter of the soil domain were restrained from displacing horizontally, while allowed to undergo settlement (z-global axis). Figure 3 also shows the point of load application that was chosen according to the field experiment (0.5 m above the soil surface). The total applied load within the model was divided into 10 load increments, where an energy convergence criterion was used with a 10^{-5} convergence tolerance.

After performing the first nonlinear pushover analysis, the areas where the pile-soil interface was found to be under tension were located. Thereafter, the soil hexahedral elements at those regions were deleted in order to detach the concrete from the soil domain. This second model was developed to further investigate the mechanical response of the specimens, where a parametric investigation of the numerical model was also performed. The initial model is referred to as the "No Gap" model, and the second model as the "Gap" model, as shown in Figure 4. It is important to note here that the concrete-soil interface that was found to be under tension extended to a depth of 3 m (i.e. 5 pile diameters).

MATERIAL PROPERTIES

The material properties adopted for the soil, concrete and reinforcement numerical models are presented in this section. It is important to note that the representative values of the Young's modulus and the compressive strength of the soil in the numerical analysis were not available from experimental tests; therefore, a parametric investigation was performed based on the values presented in Table 1. As can be seen, the values assume a minimum soil compressive strength of 89 kPa, whereas the maximum assumed uniaxial compressive strength is 150 kPa. To be able to investigate the overall response and the effect that the soil compressive strength has on the SSI system, five additional values were assumed.

Table 1 Soil input parameters

Parameter	Value	Units
Young's modulus	50, 100, 150	MPa
Compressive strength	89, 100, 110, 120, 130, 140, 150	kPa
Poisson's ratio	0.3	–

Table 2 Concrete (grey section) and steel (green section) material input parameters as determined from standard material testing

Parameter	Value	Units
Young's modulus	31.4	GPa
Uniaxial compressive strength	45	MPa
Tensional strength	2	MPa
Poisson's ratio	0.2	–
β for remaining shear strength	5	%
Elastic limit	50	%
Young's modulus	200	GPa
Poisson's ratio	0.3	–
Steel hardening	4	GPa
Steel f_y	500	MPa
Steel failure	0.12	–

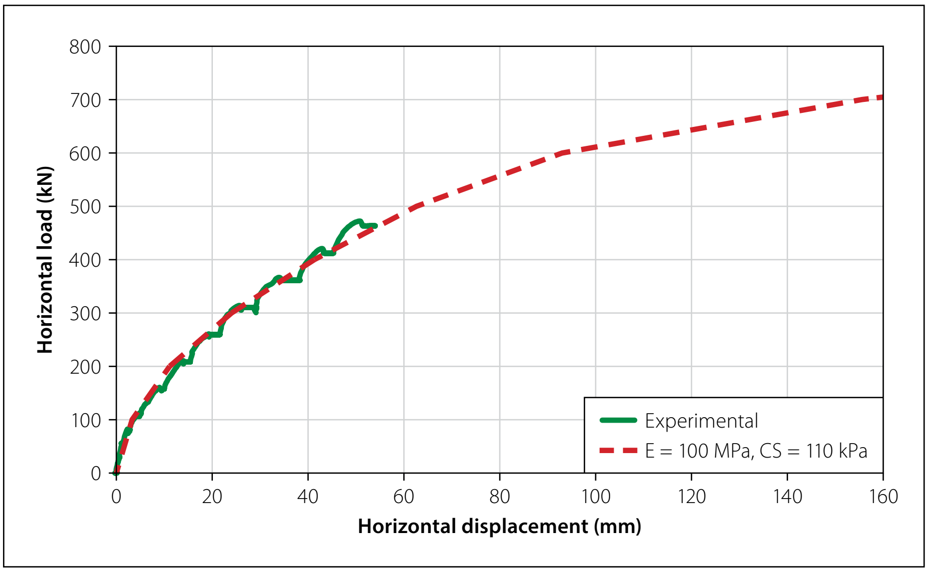

Figure 5 "Gap" model with the best fit – comparison between the numerical and experimental curves

Furthermore, three different unsaturated soil Young moduli values were investigated for the needs of this research work. The respective material properties defined for the concrete and steel rebar are presented in Table 2. It is important to note here that for both longitudinal and shear reinforcement, the yielding stress was assumed to be equal

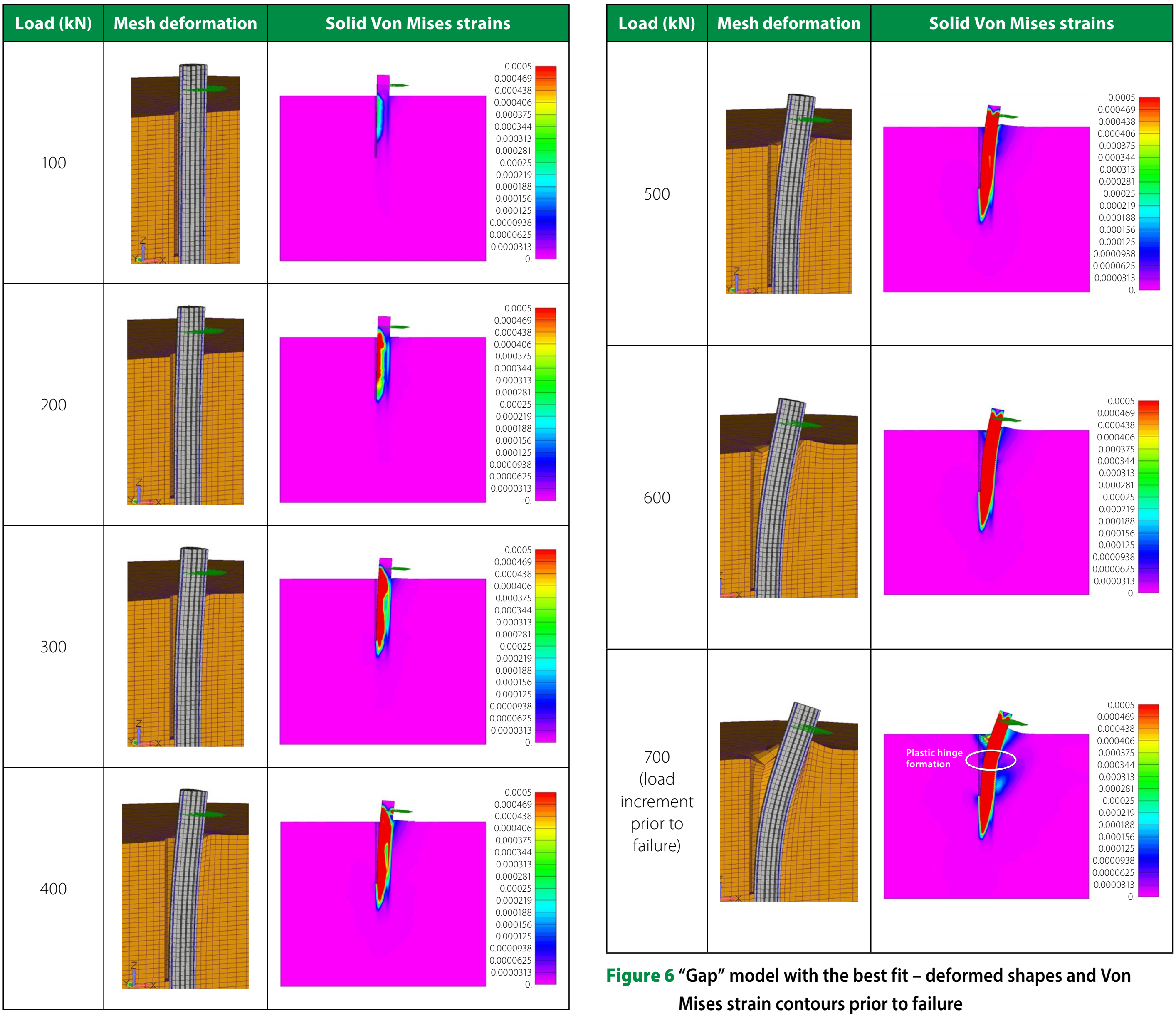

Figure 6 "Gap" model with the best fit – deformed shapes and Von Mises strain contours prior to failure

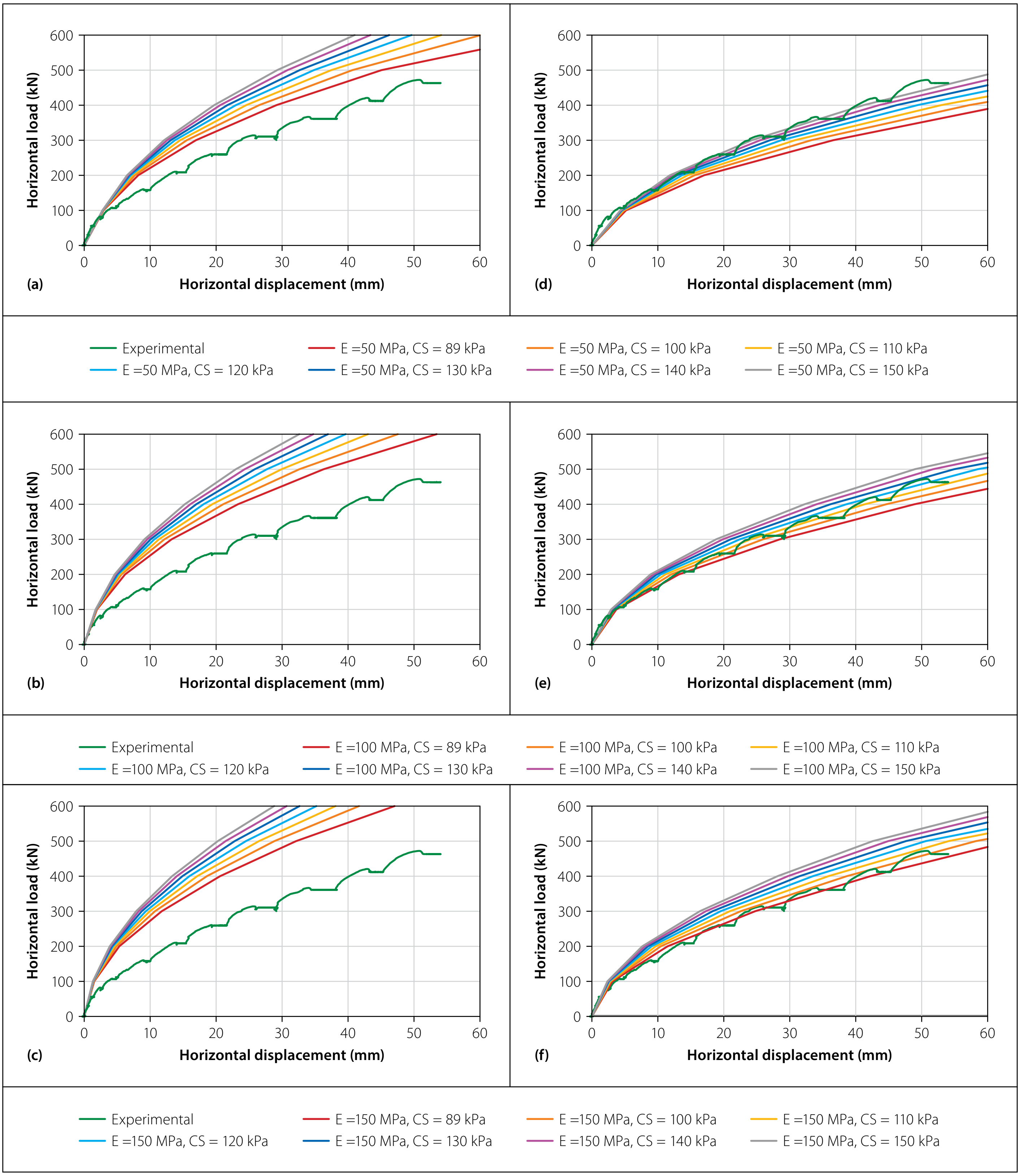

Figure 7 Horizontal load versus horizontal displacement for different soil material combinations: (a–c) "No Gap" and (d–f) "Gap" models

to 500 MPa, an average value derived from experimental tests.

NUMERICAL INVESTIGATION

For the purpose of this study, static nonlinear analyses were performed by applying a lateral load until failure. The numerical results obtained were compared to the data obtained from the field experimentation program. Both the "No Gap" and "Gap" models were analysed under the same loading conditions, while the nonlinear analysis algorithm and the corresponding parameters were kept the same.

During the physical experiment, the maximum imposed load was 500 kN, which was the load level at which the hydraulic jack reached its maximum extension; therefore, the experiment had to be terminated. Consequently, neither the RC pile nor the soil reached a full failure state, even though the deformation was larger than the allowable limit according to international design codes. For this reason, the numerical models engaged in this research study were also used to predict the physical failure mode of the specimen and the ultimate capacity that the embedded RC pile could develop. From the numerical results derived using the two numerical models ("No Gap" and "Gap"), it was found that the latter resulted in the best match to the experimental response, i.e. where the numerically derived lateral load-displacement curve best matched the experimental data (Figure 5 on p 32). The "Gap" model adopted all the experimental material parameters obtained from the experiments performed on the concrete and steel material, while a soil Young's modulus (E) of 100 MPa and a corresponding compressive strength (CS) of 110 kPa were assumed. Therefore, by reverse engineering the problem, representative soil properties were determined. Their magnitudes were found to be realistic for the in-situ soil profile.

Figure 6 (on p 32) shows the deformed shapes and the Von Mises strain contours throughout the loading phase. Specific attention is given to the last two load increments resulting from the nonlinear ultimate limit state analysis of the optimum "Gap" model. It can be seen that increasing deformation developed in the soil domain in front of the RC pile specimen, indicating a 3D compressive failure of the clay material due to excessive compressive stresses. This led to large horizontal deformations that caused the failure of the RC pile's longitudinal reinforcement, which was located in the tensile region of the circular section. As mentioned above, the physical experiment was terminated at a total horizontal applied load of 500 kN. The numerical model predicted failure to occur at a horizontally applied load of 700 kN, thus, the model allowed a failure mechanism to be observed.

In order to further investigate the numerical response of the models developed, a sensitivity analysis was performed where the Young's modulus (E_S) for the soil material was kept constant at values of 50 MPa, 100 MPa and 150 MPa respectively, while the compressive strength (CS) of the soil was varied from 89 kPa to 150 kPa (see Table 1). In Figure 7 the total imposed horizontal load versus the horizontal displacement of the pile can be seen as derived from the nonlinear analyses. A comparison with the experimental curve is also depicted.

As can be seen from Figure 7 (on p 33), the stiffness of the pile and the soil structural system decreases with increasing horizontal load, which is attributed to the damage development in the two domains. In addition, an increase in compressive strength of the soil material results in a stiffer response and hence less horizontal deformation. It can also be observed that the "No Gap" model gives a stiffer overall response attributed to the introduction of additional stiffness at the interface of the RC pile and the soil domain. Finally, it is evident that ReconanFEA (2020) was able to successfully run all of the developed models without numerical instabilities; therefore providing the required insight in relation to the local and global nonlinear mechanical behaviour of the RC pile and the soil domain.

Soil and concrete stress and strain curves for the most critically loaded elements in the model were developed to get a better understanding of the material response during load application. Figure 8 indicates the elements where the solid Von Mises stress-strain plots were generated (yellow elements for the soil and red for the pile). These elements are located in front of the pile and represent the most critically loaded elements in the numerical analysis. Figures 9 and 10 represent the stress-strain plots for the respective soil and concrete elements determined from the nonlinear analysis. For these plots, the chosen combination of a soil Young's modulus of 100 MPa and a compressive strength ranging from 89 kPa to 150 kPa was used for the soil.

Figure 9 represents the stress-strain curve for the soil element in front of the RC pile. It can be observed that each curve reaches its compressive strength value at a different strain. The slope (E) of each curve is relatively similar, whereafter plastic deformation occurs once each material has reached its ultimate compressive strength.

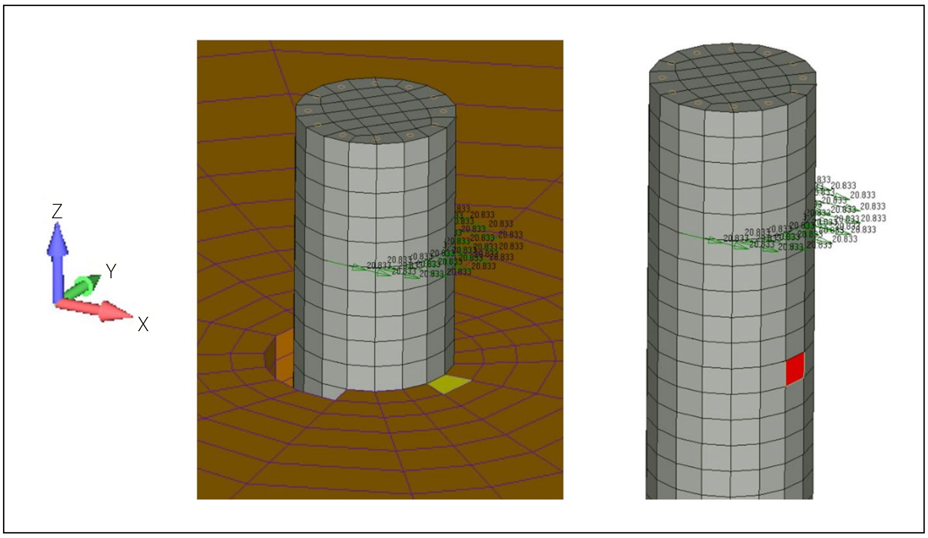

Figure 8 Element used for the soil (left) and concrete (right) stress-strain curves

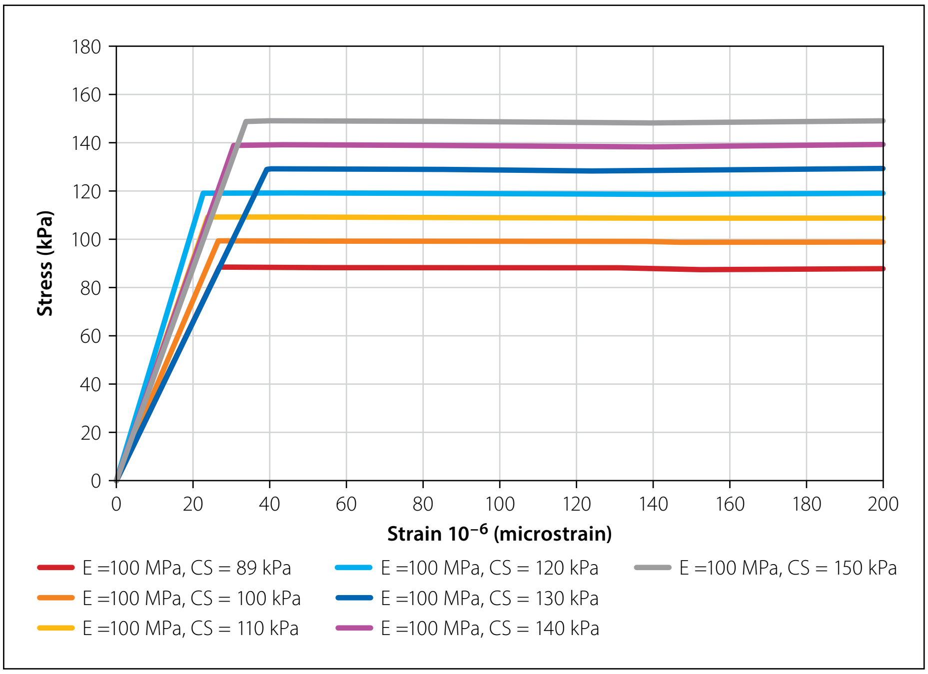

Figure 9 Stress-strain curves of the soil element in front of the pile

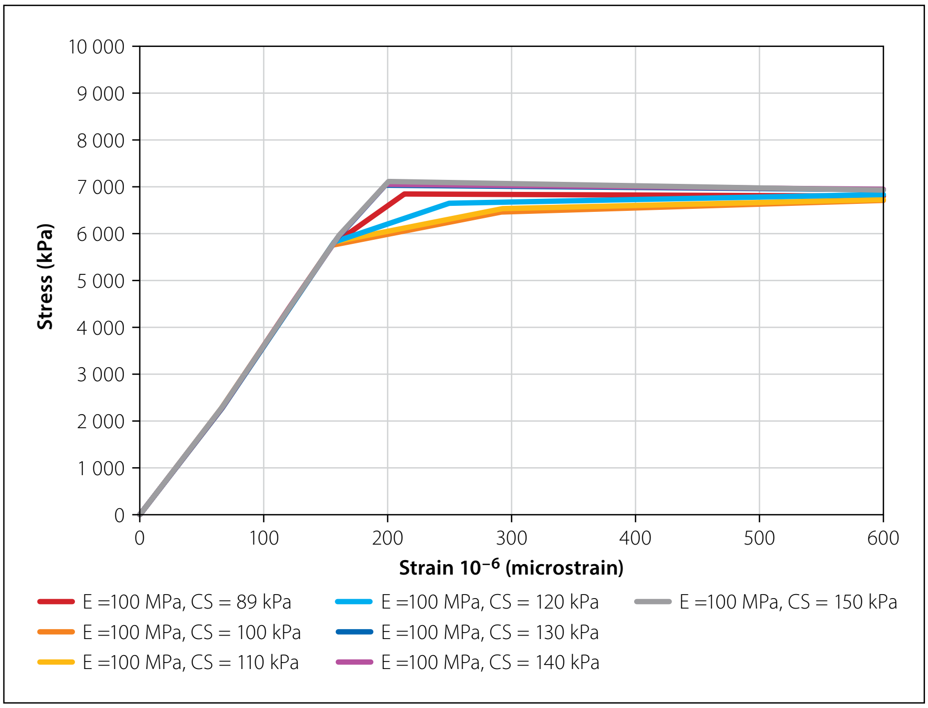

Figure 10 Stress-strain curves of the concrete element in front of the pile

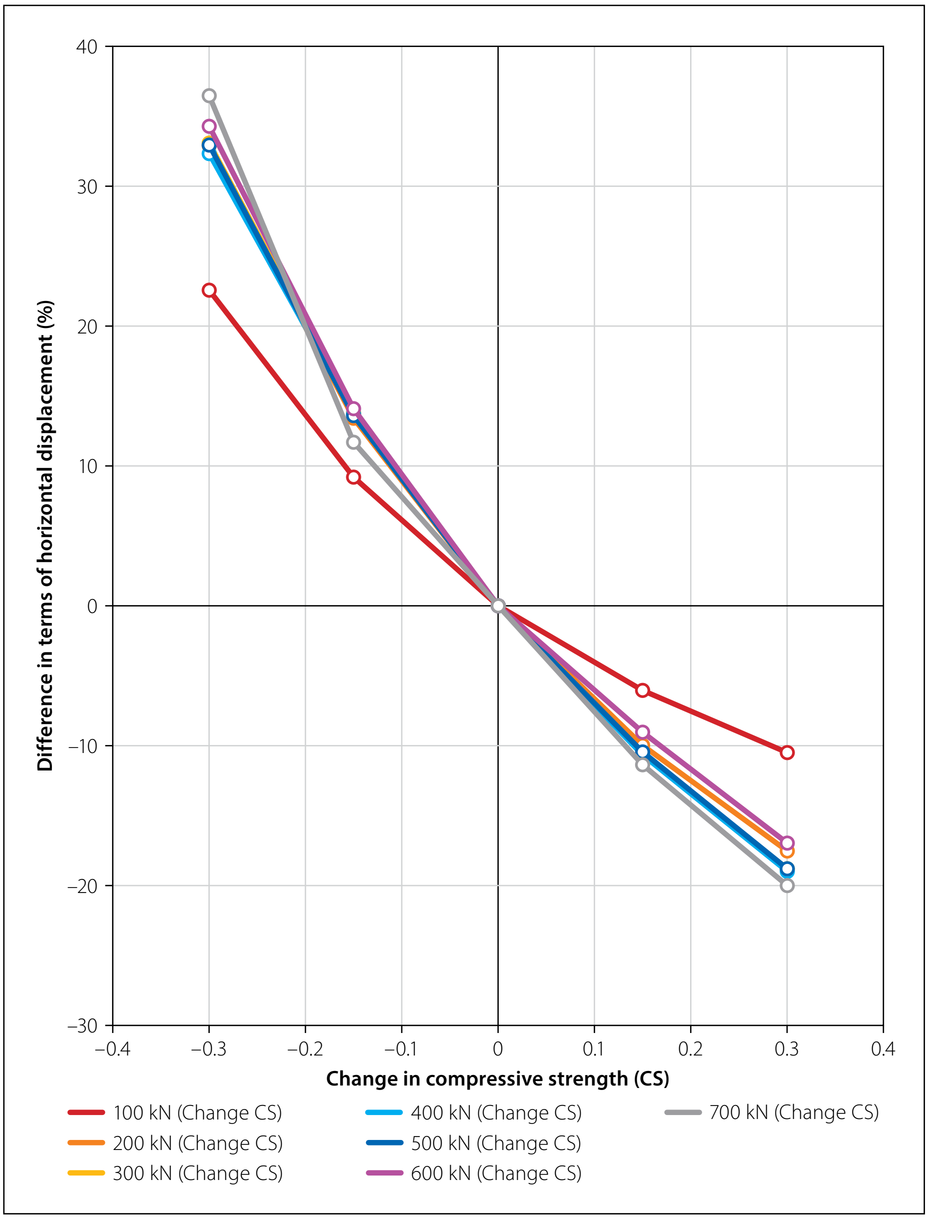

Figure 11 Sensitivity of the model due to soil compressive strength in terms of horizontal displacement

Since neither strain hardening nor strain softening occurs within the soil element, the overall mechanical response of the soil material is classified as an elastic-perfectly plastic material.

Figure 10 represents the stress-strain curves of the concrete element in front of the RC pile. It can be observed that the slope in the elastic region (E) is the same for the different compressive strength values. After the concrete has undergone elastic deformation, yielding of the concrete occurs at a specific stress, whereafter a certain magnitude of strain hardening occurs until failure. When looking at the stress magnitude in the concrete pile at failure, it can be observed that, for a lower compressive strength of the soil, a lower solid Von Mises stress develops within the concrete, while, for a higher compressive strength of the soil, a higher solid Von Mises stress develops within the concrete until significant deformation starts to occur. This phenomenon is attributed to the SSI effect, as well as to the stiffness that the soil exhibits, which is controlled by the uniaxial compressive soil strength, which in turn determines the stress level that develops within the soil domain in front of the RC pile.

PARAMETRIC INVESTIGATION

A sensitivity analysis was conducted on the parameters which could not be explicitly measured in the physical experiment. These parameters were the Young's modulus (E) and the compressive strength (CS) of the soil. For this sensitivity analysis, the "Gap" model with the same geometry, materials, constraints, loading conditions and nonlinear analysis was used. The best fit between the numerical result and the field observation resulted from using an E value of 100 MPa and a compressive strength of 110 kPa. These values were adopted as the base combination for the sensitivity analysis. This combination was used to determine how sensitive the critical parameters were to the horizontal displacement of the model for different load increments, which would also provide insight on how these parameters affect the overall mechanical behaviour of the model.

In order to illustrate the sensitivity of these parameters, the Young's modulus was kept constant, while the compressive strength was increased and decreased by 30% accordingly. Figure 11 shows the sensitivity of the model in terms of compressive soil strength and how the lateral displacement of the pile varied under different lateral load increments, ranging from 100 kN to 700 kN. Next, the compressive strength of the soil was kept constant, while the Young's modulus was assigned different values as shown in Figure 12. Figure 12 represents the sensitivity of the model in terms of horizontal displacement under different load increments, again ranging from 100 kN to 700 kN.

As can be observed in Figure 11, the higher the load, the higher the horizontal displacement difference is, compared to the initial result (best-fit curve). Therefore, as the load increases, the sensitivity of the model related to the compressive strength increases as well. In addition, a lower compressive strength in the soil is more sensitive than a higher compressive strength. Therefore, a higher compressive soil strength does not affect the model's horizontal displacement as much as a lower soil compressive strength, resulting in a model that is more sensitive for lower values. Furthermore, from Figure 12 it can be observed that a lower E value derives slightly higher differences to the model than a higher E value. It can also be seen that for any E value, the model is affected more for lower load values (100 kN). However, for a lower E value, as the load increases, the E value increase affects the model's response more for higher horizontal loads. While for a higher E value, as the load increases, the E value becomes less crucial in terms of the numerically derived horizontal displacement.

A comparison between the sensitivity of the Young's modulus (E) and the compressive strength (CS) of the soil for each load increment is given in Figure 13. It can be observed that, for an increase of the understudied parameters and at a very low load (100 kN), the Young's modulus is more crucial and affects the computed horizontal displacement more, compared to the compressive strength of the soil. However, for the remaining load increments, the soil's compressive strength is the parameter that plays the most important role in controlling the RC pile's deformation that numerically derives from the model. Therefore, the parametric investigation reveals that the overall nonlinear response of the soil domain is found to be significantly affected by both parameters, with the soil's compressive strength being the most important one.

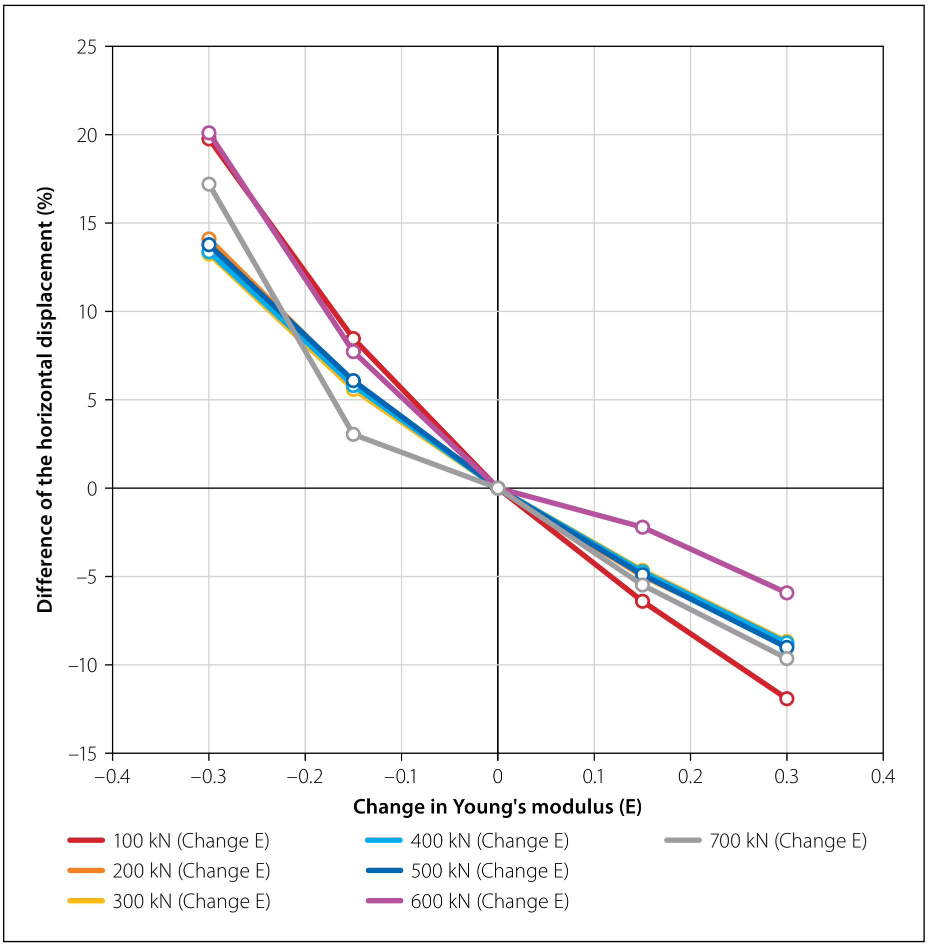

Figure 12 Sensitivity of the model due to Young's modulus in terms of horizontal displacement

CONCLUSIONS

Advanced numerical modelling and analyses were used to investigate the nonlinear mechanical behaviour of an RC pile embedded in unsaturated soil, and subjected to lateral load tests in South Africa. Two different finite element models were developed in which the material properties used in the models were based on material testing prior to the testing of the RC pile. The "Gap" model was found to provide the best fit when compared to the experimentally obtained horizontal load-displacement curve. Even though the physical experiment was not able to be loaded to failure due to equipment limitations, the numerical investigation predicted that the failure occurred due to a 3D compressive failure of the soil in front of the RC pile, which led to a bending failure of the RC pile due to large horizontal deformations.

A parametric investigation further showed that the developed numerical models were affected by the compressive strength of the soil defined within the numerical material models. It was also found that ReconanFEA, based on soil material reverse-engineered from the problem at hand, was able to successfully model the ultimate failure mechanism, allowing the actual soil properties leading to the overall mechanical response of the SSI system to be back-calculated. Finally, the software was found to be able to numerically handle the numerous nonlinear analyses that were performed without any numerical instabilities.

Future work will foresee the construction of different models, which will produce numerical results that will be used for the development of a dataset. This dataset will be used to train artificial intelligence and machine learning algorithms for the development of predictive models that will be able to estimate the expected stress and displacement levels for different RC pile geometries and soil domains.

ACKNOWLEDGEMENTS

The authors gratefully acknowledge the UK Engineering and Physical Sciences Research Council (EPSRC) Global Challenges Fund under the Wind-Africa project, Grant Ref: EP/P029434/1, for the pile load-displacement data used in this paper. This work received financial support from the EuroHPC-JU project EuroCC (G.A. 951732) of the European Commission. Parts of the runs were performed on the cyclone

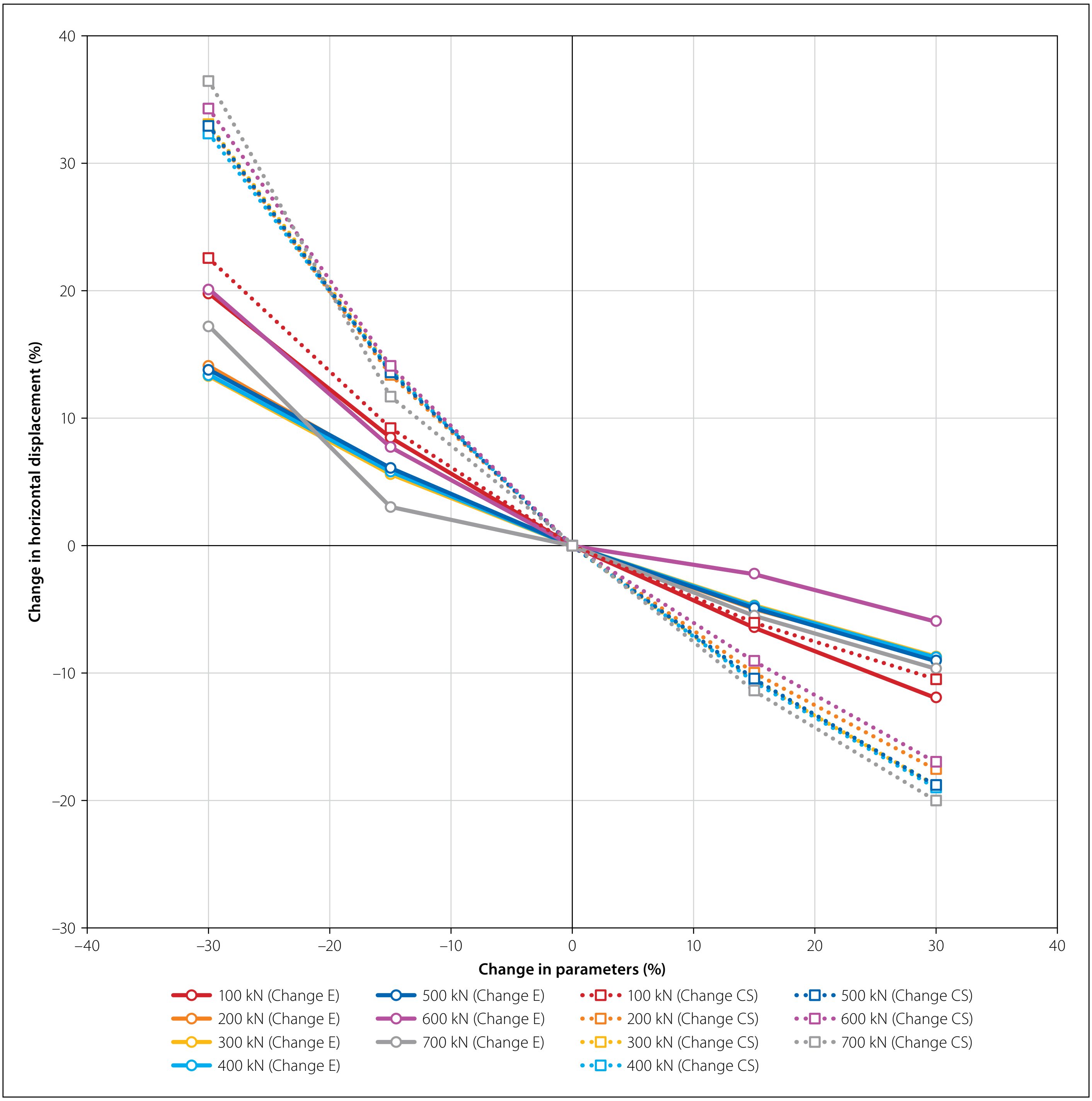

Figure 13 **Sensitivity of the E and CS on the change in horizontal displacement of the model**

machine hosted at the HPC National Competence Center of Cyprus at the Cyprus Institute (Project pro21b103).

REFERENCES

Atkinson, J 2017. *The Mechanics of Soils and Foundations*. Boca Raton, FL: CRC Press.

Breysse, D, Niandou, H, Elachachi, S & Houy, L 2005. A generic approach to soil-structure interaction considering the effects of soil heterogeneity. *Geotechnique*, 55(2): 143–150.

Červenka, J & Papanikolaou, V K 2008. Three-dimensional combined fracture-plastic material model for concrete. *International Journal of Plasticity*, 24(12): 2192–2220.

Gravett, D Z & Markou, G 2021. State-of-the-art investigation of wind turbine structures founded on soft clay by considering the soil-foundation-structure interaction phenomenon: Optimization of battered RC piles. *Engineering Structures*, 235: 112013.

Gravett, D Z, Mourlas, C, Taljaard, V-L, Bakas, N, Markou, G & Papadrakakis, M 2021. New fundamental period formulae for soil-reinforced concrete structures interaction using machine learning algorithms and ANNs. *Soil Dynamics and Earthquake Engineering*, 144: 106656.

Jardine, R, Potts, D, Fourie, A & Burland, J 1986. Studies of the influence of non-linear stress-strain characteristics in soil-structure interaction. *Geotechnique*, 36(3): 377–396.

Karthigeyan, S, Ramakrishna, V & Rajagopal, K 2006. Influence of vertical load on the lateral response of piles in sand. *Computers and Geotechnics*, 33(2): 121–131.

Kausel, E 2010. Early history of soil-structure interaction. *Soil Dynamics and Earthquake Engineering*, 30(9): 822–832.

Kavitha, P, Beena, K & Narayanan, K 2016. A review on soil-structure interaction analysis of laterally loaded piles. *Innovative Infrastructure Solutions*, 1(1): 1–15.

Kotsovos, M D & Pavlovic, M N 1995. *Structural Concrete: Finite-element Analysis for Limit-state Design*. London: Thomas Telford.

Markou, G, Alhamaydeh, M & Saadi, D 2018. Effects of the soil-structure-interaction phenomenon on RC structures with pile foundations. *Proceedings*, 9th Greek Association of Computational Mechanics

(GRACM) International Congress on Computational Mechanics. 4–6 June 2018, Chania, Greece.

Markou, G & Papadrakakis, M 2013. Computationally efficient 3D finite element modeling of RC structures. *Computers and Concrete*, 12(4): 443–498.

Markou, G & Roeloffze, W 2021. Finite element modelling of plain and reinforced concrete specimens with the Kotsovos and Pavlovic material model, smeared crack approach and fine meshes. *International Journal of Damage Mechanics*, 30(6): 845–871. doi: **10.1177/1056789520986601**.

Menegotto, M 1973. Method of analysis for cyclically loaded RC plane frames including changes in geometry and non-elastic behavior of elements under combined normal force and bending. *Proceedings,* International Association for Bridge and Structural Engineering (IABSE) Symposium on Resistance and Ultimate Deformability of Structures Acted on by Well Defined Repeated Loads. Lisbon, Portugal, pp 15–22.

Oanta, E M, Panait, C & Raicu, A 2016. Original data preprocessor for Femap/Nastran. In Vladescu, M, Panait, C T, Tamas, R, Caruntu, G & Cristea, I (Eds). *Advanced Topics in Optoelectronics, Microelectronics, and Nanotechnologies (Conference).* Vol 10010. 5–28 August 2016, Constanta, Romania. Bellingham, WA: SPIE Publications, p 1001020.

ReconanFEA v2.00. User's Manual, 2020. Available at: **https://www.researchgate.net/publication/342361609_ReConAn_v200_Finite_Element_Analysis_Software_User%27s_Manual**.